Molecular Crystals and Liquid Crystals Science and Technology. Section A. Molecular Crystals and Liquid Crystals

Publication details, including instructions for authors and subscription information:
http://www.tandfonline.com/loi/gmcl19

Control of Ct Instability In 1-D Mixed-Valence Systems

Hiroshi Okamoto [a] , Koshiro Toriumi [a c] , Tadaoki Mitani [a] & Masahiro Yamashita [b]

[a] Institute for Molecular Science, Myodaiji, Okazaki, 444, Japan

[b] Department of Chemistry, College of General Education, Nagoya University, Chikusa-ku, Nagoya, 464, Japan

[c] Department of Material Science, Himeji Institute of Technology, Harima Science Park City, Hyogo, 678-12, Japan

Version of record first published: 04 Oct 2006.

To cite this article: Hiroshi Okamoto , Koshiro Toriumi , Tadaoki Mitani & Masahiro Yamashita (1992): Control of Ct Instability In 1-D Mixed-Valence Systems, Molecular Crystals and Liquid Crystals Science and Technology. Section A. Molecular Crystals and Liquid Crystals, 218:1, 247-252

To link to this article: http://dx.doi.org/10.1080/10587259208047048

Mol. Cryst. Liq. Cryst. 1992, Vol. 218, pp. 247–252
Reprints available directly from the publisher
Photocopying permitted by license only

Printed in the United States of America

CONTROL OF CT INSTABILITY IN 1-D MIXED-VALENCE SYSTEMS

HIROSHI OKAMOTO, KOSHIRO TORIUMI,* and TADAOKI MITANI
Institute for Molecular Science, Myodaiji Okazaki 444, Japan.
MASAHIRO YAMASHITA
Department of Chemistry, College of General Education,
Nagoya University, Chikusa-ku, Nagoya 464, Japan

Abstract Control of the amplitude of CDW has been made by making use of chemical modifications in the halogen-bridged metal complexes. The dynamics of the spin soliton originated from the CT instability is discussed on the basis of the results of the ESR measurements on the complexes locating near the boundary between the mixed-valence state and the mono-valence state.

INTRODUCTION

There has been much interest in the one-dimensional (1-D) halogen(X)-bridged metal(M) complex (X = Cl, Br, I: M = Pt, Pd, Ni), because of its unique physical properties. In most of the complexes, the mono-valence state [--X^{-}----M^{3+}--X^{-}----M^{3+}--X^{-}----M^{3+}--X^{-}----M^{3+}-] is unstable due to the charge-transfer (CT) instability induced by the site-diagonal electron-lattice interaction and stabilized into the mixed-valence state, or equivalently the CDW (charge density wave) state [$\cdots X^{-}$–$M^{4\pm}$ $X^{-}\cdots\cdots M^{2\pm}\cdots X^{-}$– $M^{4\pm}$ $X^{-}\cdots\cdots M^{2\pm}\cdots$], where the bridging-halogen ion deviates from the midpoint between the neighboring metal ions (see Figure 1). Accordingly, it is an important subject to study the dynamical phenomena associated with the CT instability of the optically excited state and the ground state in these complexes.

Previously, the studies of the mixed-valence state have been made on the complexes having the large halogen distortions (e.g. $[Pt(en)_2][Pt(en)_2Cl_2](ClO_4)_4$: (en) = ethylenediamine), in which an electron or a hole excited in the chain is strongly localized by the polaron effect. In addition, the self-trapping of the CT exciton and the large stokes shift of the luminescence have been reported.[1,2]

With decrease of the halogen distortion, the electronic state approaches to the boundary between the mixed-valence state and the mono-valence state. Near the boundary, an energy of the mono-valence state (-M^{3+}–M^{3+}–) is close to that of the mixed-valence state (-M^{2+}–M^{4+}–), and then an excitation energy of an M^{3+} site in the mixed-valence state is lowered. When an M^{3+} site is excited in the mixed-valence complex near the boundary, the neighboring (-M^{2+}–M^{4+}–) mixed-valence state will become unstable by charge-fluctuation effects. That is, the CT instability is restored. ESR

*Present address: Department of Material Science, Himeji Institute of Technology, Harima Science Park City, Hyogo 678-12, Japan

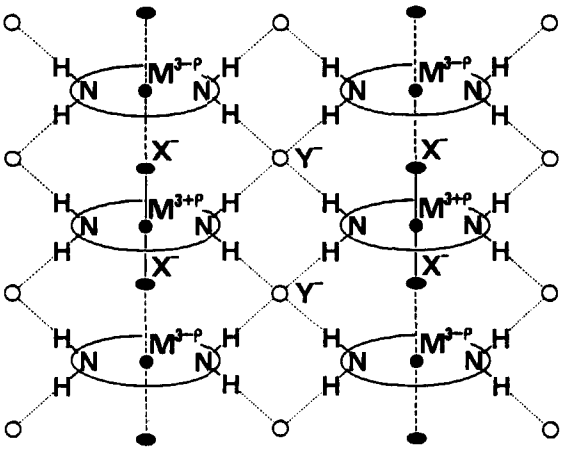

FIGURE 1 Schematic structure of the halogen-bridged metal complex. Hydrogen-bonds between the amino-groups of the ligands and the counter anions (Y^-) are shown by the dotted lines.

is a good probe to detect such M^{3+} states, since an M^{3+} site has a spin (s = 1/2). We studied the temperature dependence of ESR signals in detail in the mixed-valence complex near the boundary.

In this paper, firstly we report the chemical modifications to produce the complexes with small halogen distortions near the boundary. After that, on such complexes, we discuss the dynamical behaviors of the M^{3+} states on the basis of the results of the ESR measurements.

EXPERIMENT

The complexes $[M(chxn)_2][M(chxn)_2Br_2]Br_4$ ((chxn) = cyclohexanediamine) for M = Pd and Pt were synthesized in the same way as reported in Refs. 3 and 4. The ESR measurements were made on the single crystals with a standard Varian X-band spectrometer (E-112). The temperature of the sample was controlled by an Air-Product (LTD-3-110E) or an Oxford (ESR-9) cryogenic system. The microwave power dependence of the absorption intensity was checked at several temperatures in order to avoid saturation effects.

CONTROL OF THE CDW STATE

In Figure 2, M-X distances of l_1 ($M^{3+\rho}$-X^-) and l_2 ($M^{3-\rho}$-X^-) are plotted as a function of M-M distance L for various kinds of complexes with ethylenediamine (en) and cyclohexanediamine (chxn) as counter anions.[3,5-10] A dotted line indicates $l_1 = l_2$ which is a hypothetical line for no halogen distortions. The deviation of data of l_1 or l_2 from the dotted line corresponds to a magnitude of the halogen distortion $\Delta(=(l_2-l_1)/2)$. All data almost fall on the common curves according to the sort of the bridging-halogen ions (Br^- or Cl^-), indicating the strong correlation between Δ and L.

In Figure 2, the open marks and the solid marks show the complexes with ClO_4^- and halogen ion (Br^- or Cl^-) as the counter anion (Y^-), respectively. It is found that M-M distance L is dependent

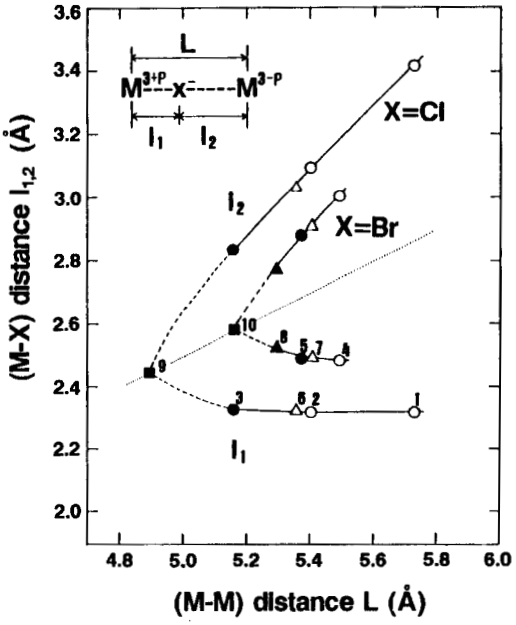

FIGURE 2 The correlation between the M-M distance (L) and the M-X distance (l_1, l_2). The data for Y = ClO_4 and halogen are represented by open and filled marks, respectively.

1:{Pt(chxn)$_2$Cl}(ClO_4)$_2$
2:{Pt(en)$_2$Cl}(ClO_4)$_2$
3:{Pt(chxn)$_2$Cl}Cl_2
4:{Pt(en)$_2$Br}(ClO_4)$_2$
5:{Pt(chxn)$_2$Br}Br_2
6:{Pd(en)$_2$Cl}(ClO_4)$_2$
7:{Pd(en)$_2$Br}(ClO_4)$_2$
8:{Pd(chxn)$_2$Br}Br_2
9:{Ni(chxn)$_2$Cl}Cl_2
10:{Ni(chxn)$_2$Br}Br_2

(1,4,7:ref.5, 2:ref.6, 3:ref.3, 5,8:ref.7, 6:ref.8, 9:ref.9, 10:ref.10)

strongly on the ligand and the counter anion. The lengths L of the complexes with Y = halogen are relatively smaller than those of the complexes with Y = ClO_4. This can be briefly explained as follows. By replacing the counter anion from ClO_4^- to the halogen ion, the hydrogen(H)-bonds between the amino-groups of the ligands and the counter anions are strengthened. Accordingly, the M-M distance L decreases and then the halogen displacement Δ effectively decreases. Among the mixed-valence complexes, the [Pd(chxn)$_2$][Pd(chxn)$_2$Br$_2$]Br$_4$ crystal (No.8 in Figure 2) has the smallest off-center displacement of the bridging-halogen ion. This complex is considered to locate near the boundary between the mixed-valence state and the mono-valence state.

Another important effect of the H-bonds to the electronic state manifests itself in the interchain interaction.[7] According to the X-ray analysis, directions of each halogen displacement are two-dimensionally ordered in the complexes with Y = halogen. (Figure 1 shows the complex having the 2-D ordering of CDW.) The 2-D ordering of CDW is hold under the presence of the 2-D tight NH-Br networks shown by dotted lines in Figure 1. In contrast, such a 2-D ordering of CDW does not exist in the complexes with Y = ClO_4. The existence of a 2-D ordering of CDW provides important modifications on the soliton excitation, as discussed below.

RESULTS AND DISCUSSIONS

The ESR measurements were made on the single crystals of [M(chxn)$_2$][M(chxn)$_2$Br$_2$]Br$_4$ for M = Pd and Pt. The results are clearly different between the two complexes. In the Pt complex, no

ESR signal was detected. On the other hand, the ESR signals of the Pd complex show a characteristic temperature dependence, as described below.

The ESR signals of the Pd complex were observed at $g_{//}=2.006$ and $g_{\perp}=2.112$ at room temperature, which can be ascribed to the paramagnetic spins ($s=1/2$) of Pd^{3+}. The temperature dependence of the integrated intensity of the ESR signals is presented in Figure 3 (a) as a double logarithmic plot [$\log_{10}(\chi_s)$-$\log_{10}(T)$]. At low temperatures below 100 K, χ_s follows the Curie law as shown by the dotted line. This indicates that a constant number of noninteracting Pd^{3+} spins exists in the 1-D chains. The concentration of the Curie spin is about 4×10^{-3} per Pd site. Above 100K, χ_s deviates from the straight line and increases with increasing temperature, suggesting that there occurs a thermal excitation of the Pd^{3+} sites. The component of the thermally excited spins $\tilde{\chi}_s$, which can be obtained by subtracting the Curie component from the observed χ_s, is presented in Figure 3 (b). The plot of $\log_{10}(\tilde{\chi}_s T)$ vs 1/T shows an approximately linear relationship down to about 75 K. The broken line in Figure 3 (b) is obtained as the activation-type formula, $\tilde{\chi}_s T = A \exp(-E_s/kT)$ with $E_s=0.032$ eV and $A=0.0037$ emu K mol^{-1}. The factor A is the high temperature limit of $\tilde{\chi}_s T$, which is related to the width of the spin excitation.[11] Adopting the simple assumption that the overlap between wave functions of spin excitations is forbidden, A is given by $\omega C/L$, where, C is the Curie constant and ω the degree of degeneracy of spin. Using that $C=0.375$ emu K mol^{-1} and $\omega=2$, the width of a spin excitation L is calculated to be about 200 Pd sites.

The ESR signals show a remarkable narrowing above 100K. This temperature is almost coincident with the temperature of beginning of thermal excitations of spin; the peak-to-peak line width ΔH_{pp} decreases from 42 G at 140 K to 20 G at 300 K for magnetic fields perpendicular to the chain axis b. This behavior can be explained by the motional narrowing effect of the thermally excited spins.

As an origin of the mobile Pd^{3+} spins, the formation of the soliton kink is presumably considered. In the previous papers, the soliton kink introduced by the phase mismatching of the CDW, as shown in Figure 4 (a), has been discussed by using the 1-D model.[12-14] In this paper, we take account of the effect of interchain interactions for the interpretation of the ESR signals of the Pd complex based upon the soliton kink model.

As mentioned in the previous section, the 2-D ordering of CDW is developed in the complexes with halogen ions as counter anions. When the halogen displacement is not so small, the 2-D ordering of CDW is stiffly locked to the lattice by a cooperation with the interchain H-bonds. In this case, soliton kinks are hardly formed in the chain. This is the case of the Pt complex, which is schematically illustrated in Figure 4 (b). On the other hand, when the halogen displacement is decreased, the phase ordering of CDW will be easily disturbed even at finite temperatures, and the CDW state is likely to become one dimensional. In such a case, the soliton kinks can be easily formed as shown in Figure 4 (c). Since the displacement of the bridging-halogen ions of the Pd complex is small as mentioned above, paramagnetic spins due to the soliton kinks might be thermally excited. The motional narrowing of the ESR signals above about 100 K suggests that the soliton kink is not bound

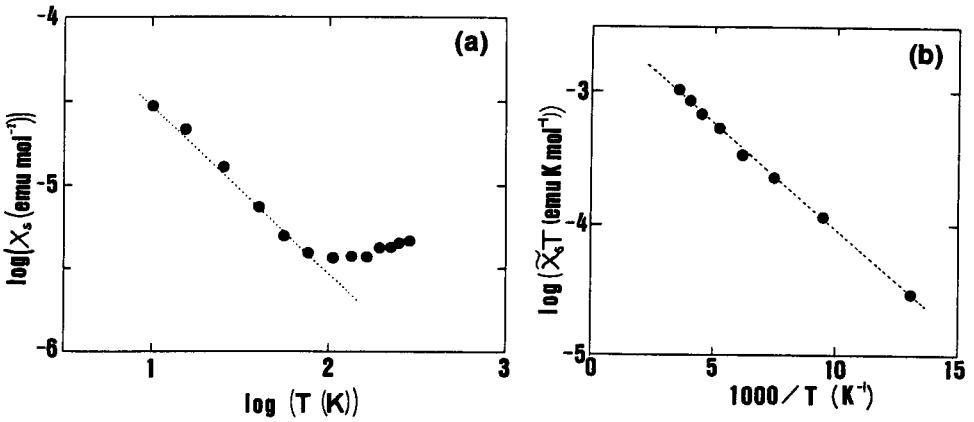

FIGURE 3 (a) Temperature dependence of the spin susceptibility χ_s of $[Pd(chxn)_2][Pd(chxn)_2Br_2]Br_4$. The dotted line represents the component following the Curie law. (b) The spin susceptibility $\tilde{\chi}_s$ for the thermally excited spin evaluated by subtracting the Curie component from χ_s.

but moves freely in the chain. While the Curie spin observed below 100 K could be attributed to soliton-like spins which are frozen at low temperatures. In the Table I, the physical data of the complexes discussed in this paper are summarized.

The width of a soliton kink L = 200 estimated above is considerably large. Such a large value of L suggests that the spin soliton kink might become stable to be expanded to the Pd^{3+} domain as shown by the broken line in Figure 4 (c), since the energy of the mono-valence state is close to that of the mixed-valence state in this Pd complex.

Finally, let us compare the magnetic property of the $[Pt(chxn)_2][Pt(chxn)_2Br_2]Br_4$ complex with that of the $[Pt(en)_2][Pt(en)_2I_2](ClO_4)_4$ complex. These two complexes have almost the same magnitudes of the halogen distortions ($d = 2\Delta/L$) and the CT excitation energies, as listed in Table I.[2,5,7] As previously reported, the ESR signals of Pt^{3+} spins have been detected in the $[Pt(en)_2][Pt(en)_2I_2](ClO_4)_4$ complex.[15] The concentration of Pt^{3+} spins in this complex was estimated to be about 10^{-4} per Pt site and found to be constant below the room temperature. The concentration of Pt^{3+} spins of $[Pt(chxn)_2][Pt(chxn)_2Br_2]Br_4$ is at least 1 order of magnitude smaller than that of $[Pt(en)_2][Pt(en)_2I_2](ClO_4)_4$. In the case of $Y = ClO_4$, the H-bond network is considerably weak and the CDW chain is one-dimensional in character, so that the soliton-like Pt^{3+} defects are easily introduced in the 1-D chains possibly during the crystallization process. Thermal excitations of the spin soliton could not occur due to their high excitation energy.

We are grateful to Prof. R. Ikeda (Tsukuba Univ.), Mr. M. Iida (Nagoya Univ.), Dr. K. Awaga, Dr. K. Iwano and Prof. K. Nasu (IMS) for many enlightening discussions.

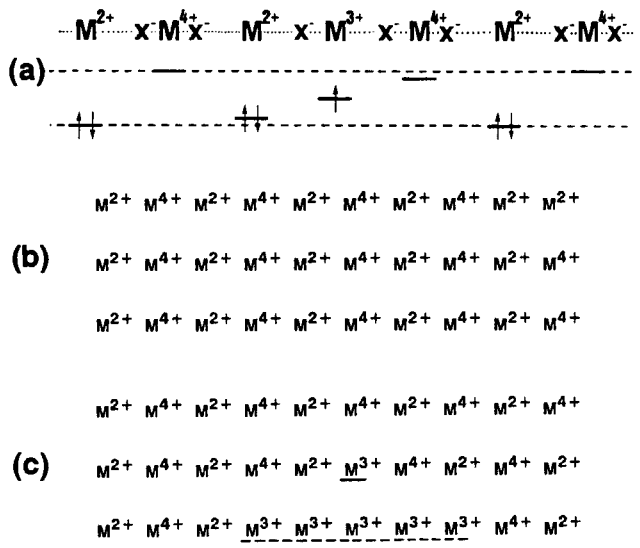

FIGURE 4 (a) Schematic structure of the spin-soliton. (b) 2-D ordering of the CDW. (c) Possible excitation of the spin (s = 1/2) states.

TABLE I Physical data for the related complexes.

	ESR signals [M^{3+}: s = 1/2]	2-D ordering of CDW	Halogen displacements (d = 2Δ/L)	CT excitation energies (eV)
$[Pd(chxn)_2]$ $[Pd(chxn)_2Br_2]Br_4$	large	weak	0.047	0.75
$[Pt(chxn)_2]$ $[Pt(chxn)_2Br_2]Br_4$	——	strong	0.073	1.40
$[Pt(en)_2]$ $[Pt(en)_2I_2](ClO_4)_4$	small	——	0.063	1.38

References

1. H. Tanino and K. Kobayashi, J. Phys. Soc. Jpn., 52, 1446 (1983).
2. Y. Wada et al., J. Phys. Soc. Jpn., 54, 3143 (1985).
3. K.P. Larsen and H. Toftlund, Acta Chem. Scand., A31, 182 (1977).
4. H. Toftlund et al., Chem. Phys. Lett., 142, 286 (1987).
5. K. Toriumi et al., unpublished results.
6. N. Matsumoto et al., Mem. Fac. Sci. Kyushu Univ., Ser C11, 209 (1982).
7. H. Okamoto et al., Phys. Rev., B42, 10381 (1990).
8. A.L. Beauchamp et al., Acta Cryst., B38, 1158 (1982).
9. K. Toriumi et al., Mol. Cryst. Liq. Cryst., 181, 333 (1990).
10. K. Toriumi et al., J. Am. Chem. Soc., 111, 2341 (1989).
11. K. Awaga et al., Solid State Commun., 71, 1173 (1989).
12. N. Kuroda et al., Phys. Rev. Lett., 58, 2122 (1987).
13. M. Sakai et al., Phys. Rev., B40, 3066 (1989).
14. N. Kuroda et al., J. Phys. Soc. Jpn., 59, 3049 (1990).
15. A. Kawamori et al., J. Phys. C, 18, 5487 (1985).